JOURNAL OF SPACECRAFT AND ROCKETS
Vol. 45, No. 6, November–December 2008

Stability Analysis of Beagle2 in Free-Molecular and Transition Regimes

Madhat M. Abdel-jawad,* Mark J. Goldsworthy,† and Michael N. Macrossan‡
University of Queensland, Brisbane, Queensland 4070, Australia

DOI: 10.2514/1.37034

On 25 December 2003, Beagle2, a passively controlled planetary entry vehicle, began its entry and descent into the Martian atmosphere. It was declared lost by the European Space Agency in January 2004. In this paper, we present the results of a series of direct simulation Monte Carlo simulations to calculate the aerodynamic coefficients of the aeroshell at selected points in the free-molecular and transition regimes. The aerodynamic coefficients arising from the direct simulation Monte Carlo calculations were then used as inputs for a dynamic analysis of the capsule over the first 25.4 s of its Martian entry. Our results show that it is unlikely that Beagle2 could have traced its nominal trajectory successfully due to static instability in the free-molecular regime and reduced static stability in the transition regime. This reduction in static stability was brought on by a large skin friction contribution to the pitching moment. The net moment, which is the difference between the stabilizing moments due to pressure forces and the destabilizing moments due to skin friction, is less than 0.5% for both. The high prescribed spin rate based on moments derived from a bridging function, which were significantly higher than those shown by our calculations, counteracted not only the destabilizing moments in the free-molecular regime, but also the stabilizing moments in the transition regime.

I. Introduction

THE study presented in this paper represents the first set of direct simulation Monte Carlo (DSMC) calculations of the aerodynamic coefficients for the aeroshell of Beagle2 in the first 25.4 s of its nominal trajectory. This study was conducted after the flight and the aerodynamic coefficients are used here in a dynamic analysis to assess the stability of the craft in the free-molecular and transition regimes.

Based on the relative importance of the terms in the Burnett equations, Tsien [1] showed that supersonic flow is rarefied when the parameter $M_\infty/\sqrt{Re_\infty}$ is greater than approximately 1. For $M_\infty/\sqrt{Re_\infty} < 1$, the flow is termed a transition flow (Tsien termed it slip flow [1]). Tsien's parameter is approximately equal to $\sqrt{B_\infty}$, where $B_\infty = Kn_\infty M_\infty$ is termed the freestream "breakdown parameter" [2]. Thus, for $Kn_\infty M_\infty > 1$, the flow is in the transition regime. For Beagle2 the Mach number over the analysis window was approximately constant at $M_\infty \approx 30$, so that the flow can be considered within the transition regime at $Kn_\infty < 1/30$. Tsien [1] also showed that flow is free molecular when $M_\infty/Re_\infty > 1$ (approximately), that is, when the Knudsen number is approximately greater than unity.

The planned flight of Beagle2 [3] through the Martian atmosphere followed a trajectory of decreasing rarefaction, that is, decreasing Knudsen number (Kn). Hence, Beagle2 encountered the free-molecular regime ($Kn > 1$) and then the transition regime ($Kn \sim 1- \sim 0.03$) before its entry into the continuum regime ($Kn < 0.001$). Planetary entry capsules are often unstable in the free-molecular regime. Hence, the transition regime is crucial in restoring trim. In transition and free-molecular hypersonic flow, the surface shear stress accounts for more than 80% of the forces on the body [4]. A significant destabilizing surface friction contribution to aerodynamic moments has been demonstrated in the free-molecular and transition regimes [4]. For example, Stardust underwent a trajectory design change when calculations showed that trim restoration in the transition regime could not be achieved [5].

Because of financial constraints, the Beagle2 aerodynamic coefficients were calculated before launch based on a blended database that relied on a bridging function to characterize the moment coefficients in the free-molecular and transition regimes.

We report results of a stability analysis for Beagle2 in the free-molecular and transition regimes. We calculated the aerodynamic moments at various angles of incidence using three-dimensional DSMC simulations for steady flow conditions along the nominal trajectory of Beagle2. The Knudsen number ranged from $Kn = 3.29$ to 0.0291, corresponding to times of 0–25.4 s after (nominal) atmospheric entry. These simulations were of reacting (59 reactions) nonequilibrium Martian atmosphere flows modeled as 95%CO_2 and 5%N_2.

We then carried out an Euler angle dynamic analysis using the moments obtained from our DSMC calculations. The analysis time window included a condition ($Kn = 0.2846$, time = 13.2 s) along the nominal trajectory of Beagle2 where zero incidence had been targeted.

II. Numerical Methods

A. Direct Simulation Monte Carlo Calculations

We used the DSMC method [6] to calculate the aerodynamic coefficients for noncontinuum flow using version 2.5 of the DS3V program of Bird [7].

Simulations were conducted at the conditions listed in Table 1 and represented the first 25.4 s of the entry and descent of the capsule. A total of 59 chemical reactions were simulated using the total collision energy chemistry model as defined by Bird [7]. The species used are listed in Table 2. For this set, the total collision cross-sectional area was given by $\sigma_T = \pi d_{\text{ref}}^2 (g_{\text{ref}}/g)^{2\omega-1}$, where $g_{\text{ref}}^{2\omega-1} = (2kT_{\text{ref}}/m')^{\omega-0.5}/\Gamma(2.5-\omega)$, $T_{\text{ref}} = 273$ K, ω is the viscosity exponent, m' is the reduced mass, k is the Boltzmann constant, and $Z_v = (C_1/T^\omega)\exp(C_2 T^{-1/3})$ is the vibrational relaxation rate equation. All reflecting surfaces were modeled as diffuse reflectors with complete accommodation in the velocity components and in the rotational energy.

A set of 59 chemical reactions used in the simulations are shown in Table 3. The chemical reactions were modeled to match the Arrhenius reaction rate according to $k_f = A_r T^\eta \exp(E_a/kT)$ m^3/s.

Received 7 February 2008; revision received 26 May 2008; accepted for publication 29 May 2008.

*Lecturer, Centre for Hypersonics, School of Engineering.
†Senior Lecturer.
‡Postgraduate Student.

Table 3, for brevity, lists the terms A, B, W, X, Y, and Z. Here they represent different sets of reactants according to

$$A = O_2, N_2, NO, CO, CO_2; \qquad B = O, N, C$$

$$W = O_2, N_2, NO, CO, CO_2, C, Ar; \qquad X = O, N$$

$$Y = O, N, NO, C, CO_2; \qquad Z = O_2, N_2, CO, Ar$$

B. Direct Simulation Monte Carlo Calculations

Computational verification of the reliability of the results was obtained by a particle-dependence study for the 25.4 s flight condition, the details of which are given herein.

We used the code's built-in eight-species Martian atmosphere model with the default variable hard sphere collision cross sections (as defined by Bird [7]) and the constant rotational and variable vibrational relaxation collision numbers. The computational domain

Table 1 Conditions modeled along the nominal trajectory of Beagle2

ζ, deg	Time, s	Rho, kg/s	Number density, m^{-3}	Wall Temp., K	U, m/s	V, m/s	W, m/s	T, K
2	13.2	1.98E − 07	2.76E + 18	300	5.41E + 03	0	188.871	141.6
5	13.2	1.98E − 07	2.76E + 18	300	5.39E + 03	0	471.6743	141.6
11	13.2	1.98E − 07	2.76E + 18	300	5.31E + 03	0	1032.6	141.6
16.5	13.2	1.98E − 07	2.76E + 18	300	5.19E + 03	0	1537.1	141.6
2	19.3	6.51E − 07	9.07E + 18	700	5.41E + 03	0	189.0499	144.8
5	19.3	6.51E − 07	9.07E + 18	700	5.40E + 03	0	472.1209	144.8
11	19.3	6.51E − 07	9.07E + 18	700	5.32E + 03	0	1033.6	144.8
16.5	19.3	6.51E − 07	9.07E + 18	700	5.19E + 03	0	1537.1	144.8
2	25.4	2.01E − 06	2.80E + 19	1000	5.42E + 03	0	189.1815	149.2
5	25.4	2.01E − 06	2.80E + 19	1000	5.40E + 03	0	472.4495	149.2
11	25.4	2.01E − 06	2.80E + 19	1000	5.32E + 03	0	1034.3	149.2
16.5	25.4	2.01E − 06	2.80E + 19	1000	5.19E + 03	0	1537.1	149.2

Table 2 Species used in the simulation of the Martian atmosphere

	Species	Diameter d_{ref}, A	Viscosity exponent ω	Rotational collision number	Vibrational temperature, K	Vibrational relaxation rate constants C_1	Vibrational relaxation rate constants C_2
1	O_2	4.07	0.77	5	2256	56.5	153.5
2	N_2	4.17	0.74	5	3371	9.1	220
3	O	3.00	0.80	——	——	——	——
4	N	3.00	0.80	——	——	——	——
5	NO	4.20	0.79	5	2719	37.7	175
6	C	2.72	0.80	——	——	——	——
7	CO	4.19	0.73	5	3103	37.7	175
8	CO_2	5.62	0.93	8	1997	1618.4	70.85
					960	25.48	177.98
					960	25.48	177.98
					3380	7.9E − 3	386.5
9	Ar	4.17	0.81	——	——	——	——

Table 3 Reactions used in the simulation of the Martian atmosphere

Number	Reaction	A_r	η	E_a, K	Reaction energy, K
1–9	$CO_2 + M \rightarrow CO + O + M$	6.144E − 16	0	−52500	−52500
10–18	$CO + M \rightarrow C + O + M$	3.819E − 11	−1	−129000	−129000
	$N_2 + A \rightarrow 2N + A$	1.162E − 08	−1.6	−113200	−113200
19–27	$N_2 + B \rightarrow 2N + B$	2.490E − 08	−1.5	−113200	−113200
	$N_2 + Ar \rightarrow 2N + Ar$	5.812E − 09	−1.5	−113200	−113200
28–36	$O_2 + W \rightarrow 2O + W$	3.321E − 09	−1.5	−59500	−59500
	$O_2 + X \rightarrow 2O + X$	1.606E − 09	−1.5	−59500	−59500
37–45	$NO + Y \rightarrow N + O + Y$	1.826E − 13	0	−75500	−75500
	$NO + Z \rightarrow N + O + Z$	8.303E − 15	0	−75500	−75500
46	$CO_2 + O \rightarrow O_2 + CO$	4.218E − 19	0.5	−27690	−4066
47	$CO + N \rightarrow NO + C$	4.750E − 19	0.5	−53620	−53320
48	$2CO \rightarrow CO_2 + C$	3.869E − 21	0.5	−65700	−65300
49	$CO + O \rightarrow O_2 + C$	4.533E − 18	0.5	−69530	−69360
50	$N_2 + O \rightarrow NO + N$	1.220E − 18	0.5	−37930	−37770
51	$NO + CO \rightarrow CO_2 + N$	7.620E − 12	0.5	−12060	−11980
52	$NO + O \rightarrow O_2 + N$	4.218E − 19	0.5	−23370	−4066
53	$O_2 + CO \rightarrow CO_2 + O$	8.302E − 22	1	−23900	4066
54	$NO + C \rightarrow CO + N$	4.317E − 20	0.5	0	53310
55	$CO_2 + C \rightarrow 2CO$	7.638E − 18	−0.25	0	65290
56	$O_2 + C \rightarrow CO + O$	1.561E − 20	0.25	0	69360
57	$NO + N \rightarrow N_2 + O$	2.657E − 19	0.5	0	37770
58	$CO_2 + N \rightarrow NO + CO$	1.644E − 07	−0.25	0	11980
59	$O_2 + N \rightarrow NO + O$	1.577E − 20	1	0	16050

Table 4 DS3V grid sensitivity study results; Beagle2 simulation at an 82.5 km altitude and a 2 deg AOA ($M_\infty = 25.3$, $Kn_\infty = 0.03$)

Case	Starting MB	Simulation particles	F_x	F_z	M_y
1	100	290,000	16.05	0.383	0.010
2	200	581,000	15.98	0.375	0.012
3	300	870,000	15.94	0.376	0.011
4	400	1,160,000	15.92	0.367	0.011
5	600	1,730,000	15.89	0.370	0.014
6	800	2,320,000	15.88	0.368	0.014
7	800	11,600,000	15.88	0.367	0.014

consisted of a rectangular flow region surrounding a 3-D model of the Beagle2 aeroshell. The symmetry axis of the aeroshell lay along the x axis with the nose located at the xyz coordinates (0, 0, 0). The pitching motion of the capsule occurred in the x–z plane. A symmetry boundary at $y = 0$ passed through the center of the capsule. The bounding box of the domain was (X: $-0.6, 1.0$; Y: 0.0, 1.4; Z: $-1.4, 1.4$) m. The freestream conditions corresponded to those at a flight time of 25.4 s at an 82.5 km altitude and a 2 deg angle of attack. The density was 2.01×10^{-6} kg/m^3, the speed 5421 m/s, and the temperature 149 K. The freestream was modeled as 95%CO_2 and 5%N_2.

Seven simulations were run (listed in Table 4) with varying numbers of simulation particles. The table gives the number of starting megabytes, which controls how much memory is devoted to the automatically constructed computational cells. In cases 1–6, the collision cell sizes were adapted to contain an average of eight simulator particles, and the sampling cells an average of 30 particles. The DS3V code would not construct a finer mesh than that in case 6. Hence, for the final simulation case, the total number of simulation particles was increased by a factor of 5 over case 6, yet the same cell sizes were used. Because potential colliding particle pairs are selected with a bias toward nearest neighbors, using more simulator particles in each cell is similar in some ways to using a finer mesh.

Net forces and moments (about the point $xyz = 0.2363, 0, 0$) for each case are shown in Table 4. Convergence toward values of F_x, F_z, and M_y that are independent of the number of simulation particles is apparent. Similar convergence behavior is expected for all the Beagle2 flight conditions.

C. Dynamic Model

Because the aeroshell is axisymmetric, the aerodynamic problem can be expressed in terms of a single compound angle of incidence, ζ. In our dynamic analysis, the instantaneous angles of attack (α) and sideslip (β) determine the angle of incidence (ζ) at which the aerodynamic moments were interpolated from our DSMC results and resolved into the yawing and pitching moments in the inertial frame of reference.

The aeroshell of Beagle2 is an axisymmetric 60 deg half-angle sphere cone. The mass distribution of Beagle2 is not axisymmetric, but the nondiagonal terms in the inertia matrix are 2 orders of magnitude less than the diagonal terms. These nondiagonal terms were set to 0 and moments were resolved about the on-axis reference point of Beagle2 located 0.2363 m behind the nose tip.

A MATLAB® Simulink dynamic model was constructed using the moments from the DSMC calculations as the excitation. A database of moments obtained from the DSMC calculations in the plane of ζ was constructed. The flow time and the instantaneous values of α and β were first used to calculate ζ; the moments were resolved into y and z components based on α and β. The Euler angles were then solved using the following equation [8]:

$$\begin{bmatrix} \ddot{\phi} \\ \ddot{\alpha} \\ \ddot{\beta} \end{bmatrix} = \begin{bmatrix} Ixx & 0 & 0 \\ 0 & Iyy & 0 \\ 0 & 0 & Izz \end{bmatrix}^{-1} \left(\begin{bmatrix} 0 & -\dot{\beta} & \dot{\alpha} \\ \dot{\beta} & 0 & -\dot{\phi} \\ -\dot{\alpha} & \dot{\phi} & 0 \end{bmatrix} \cdot \begin{bmatrix} Ixx & 0 & 0 \\ 0 & Iyy & 0 \\ 0 & 0 & Izz \end{bmatrix} \begin{bmatrix} \dot{\phi} \\ \dot{\alpha} \\ \dot{\beta} \end{bmatrix} + \begin{bmatrix} Mxx \\ Myy \\ Mzz \end{bmatrix} \right) \tag{1}$$

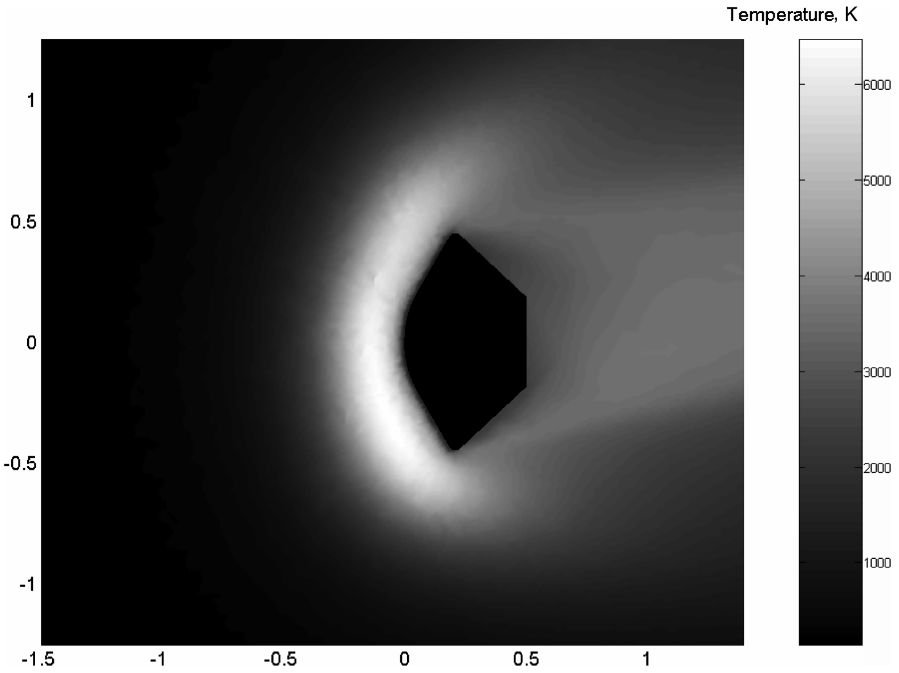

Fig. 1 Plane of symmetry view of the DSMC results of the overall temperature field around Beagle2 at $Kn = 0.0291$ and an 11 deg incidence.

where $\dot{\phi}$, $\dot{\alpha}$, and $\dot{\beta}$ are the angular velocities; $\ddot{\phi}$, $\ddot{\alpha}$, and $\ddot{\beta}$ are the angular accelerations with respect to the inertial frame of reference; M_p is the moment; and I_p the moment of inertia about the p axis. Having found the instantaneous accelerations $\ddot{\phi}$, $\ddot{\alpha}$, and $\ddot{\beta}$ from Eq. (1), the subsequent instantaneous angular velocities can be found by integration. Similarly, the subsequent instantaneous angular positions ϕ, α and β can be can be found by integrating the instantaneous angular velocities $\dot{\phi}$, $\dot{\alpha}$, and $\dot{\beta}$. A MATLAB® ODE23 solver was used for these operations.

III. Results and Discussion

The output of the DSMC calculations was flowfield solutions that included temperatures, velocities, densities, species mass fractions, surface pressure, and surface friction forces. The surface forces were integrated to provide the net axial, normal, and side forces, as well as the moments about the three axes, acting on the aeroshell.

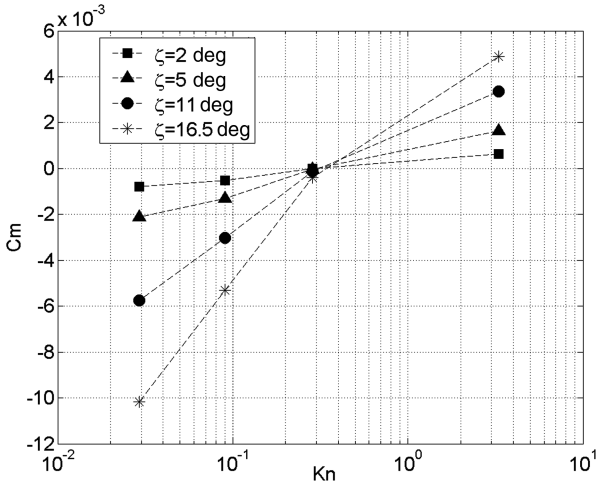

Fig. 2 Moment coefficients for Beagle2 at an incidence for $Kn = 3.29$–0.0291. Positive values indicate static instability. $L_c = 0.924$ m.

Temperatures in a significant portion of the merged layer exceeded 6000 K (Fig. 1), but little dissociation behind the bow shock is seen. Instead, nearly all concentration polarization is due to the relative differential diffusion of species. The aerodynamic phenomena observed are therefore nearly decoupled from the chemical kinetic effects.

Static stability can be characterized by the moment coefficient C_m, which is given by

$$C_m = \frac{M}{\frac{1}{2}\rho_\infty u_\infty^2 A_c L_c} \tag{2}$$

where M is the moment, ρ_∞ is the freestream density, u_∞ is the freestream velocity, A_c is the characteristic area, and L_c is the characteristic length. The characteristic length used here was 0.924 m and the characteristic area was that of a circle with diameter equal to L_c. Values of the moment coefficient C_m are shown in Fig. 2.

Our DSMC results (Fig. 2) show static instability characterized by a positive moment coefficient, $C_m > 0$, at the most rarefied condition (time = 0 s, $Kn = 3.29$). The results also show that, at the target 0 angle of attack condition, Cm is near 0 for all values of ζ. At this condition, the surface friction contribution to the moment (destabilizing) is nearly equal to the pressure contribution (stabilizing). The net moment, which is the difference between the surface friction and pressure contributions, is less than 0.5% for both.

Figure 3 shows the results for α and β from our dynamic analysis starting at $\alpha = 2$, 5, 7, 9, 11, and 16 deg and $\beta = 0$ deg, whereas Fig. 4 shows the results for $\beta = 2, 5, 7, 9, 11$, and 16 and $\alpha = 0$ deg. The results show that Beagle2 could not have recovered from any of the starting conditions over the entire analysis time window from angles of attack as high as 16 deg, and that the angle of attack is increased if the starting incidence is purely sideslip. Far from being a damped system, the entry and descent of a capsule into a planetary atmosphere is subject to continual excitation by the gravitational pull of the planet, which leads to greater oscillations in both the angle of attack and sideslip, as seen in Figs. 3 and 4.

The phenomenon seen in Figs. 3 and 4 whereby the capsule does not recover from its initial angle of attack arises due to a high spin rate (85.2 deg/s), which serves to reduce the effect of destabilizing moments in the free-molecular regime but hinders trim angle

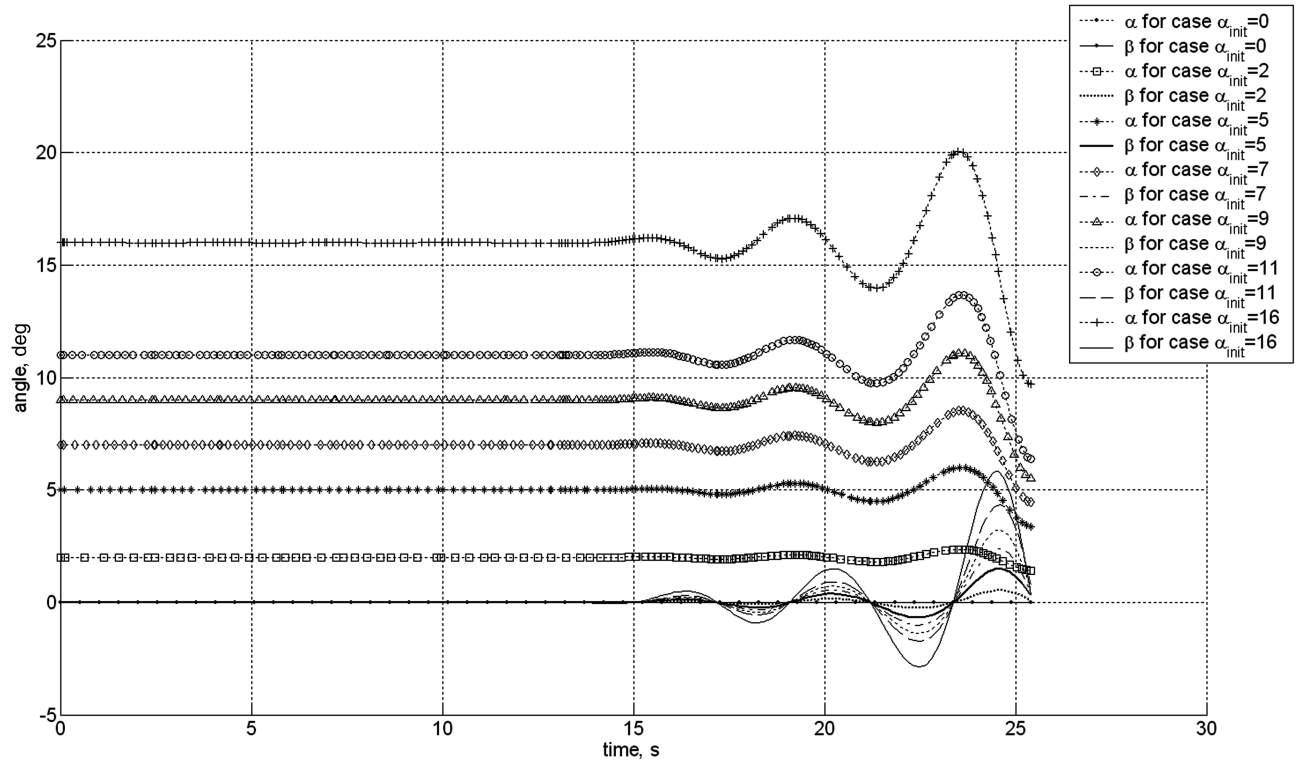

Fig. 3 Time histories of angles of attack and sideslip for cases in which $\alpha_{init} = 0$–16 deg and $\beta_{init} = 0$.

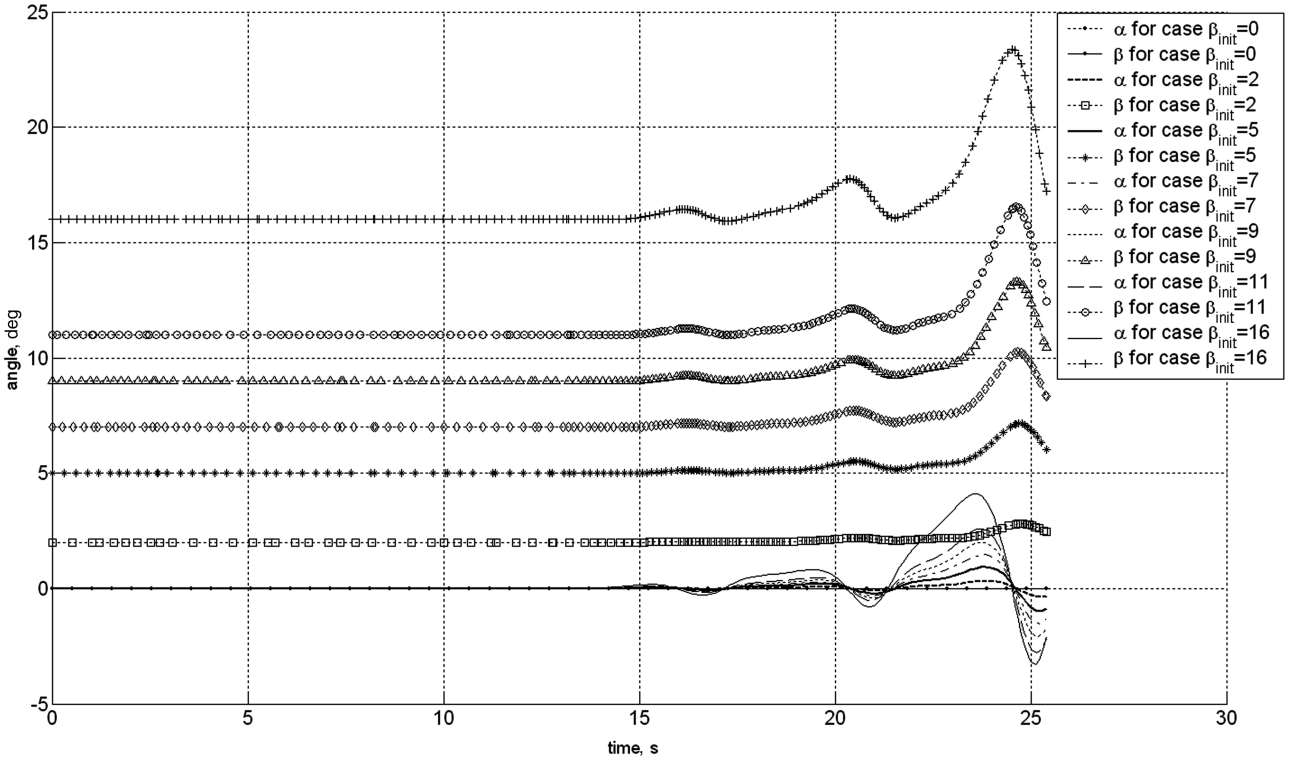

Fig. 4 Time histories of angles of attack and sideslip for cases in which $\beta_{\text{init}} = 0$–16 deg and $\alpha_{\text{init}} = 0$.

recovery by counteracting the smaller than expected stabilizing moments in the transition regime. It results in the craft not deviating from its initial orientation, which was about 16 deg.

The reason for this can be seen in Fig. 5, which shows the instantaneous angle of attack normalized by the initial angle of attack for angles of attack of 2, 7, and 16 deg (the results for the other angles of attack fall in between those shown). The figure shows the results for the Beagle2 flight and a flight along the same trajectory but with no spin about the axis of symmetry. The figure shows that the 85.2 deg/s spin hinders trim angle recovery.

The value of the angles of attack and yaw in Figs. 3 and 4 are diminishing toward the end of the analysis time window. However, the magnitude of the derivatives of some of the curves in Figs. 3 and 4 are also reducing, indicating a potential subsequent rise in the angles of attack and yaw. This would be consistent with an anticipated increase in the amplitude of oscillation about a relatively constant mean value, although further analysis at higher densities is required to verify this. In any case, the work presented in this paper alone cannot be taken as evidence that the capsule was unstable in the continuum regime.

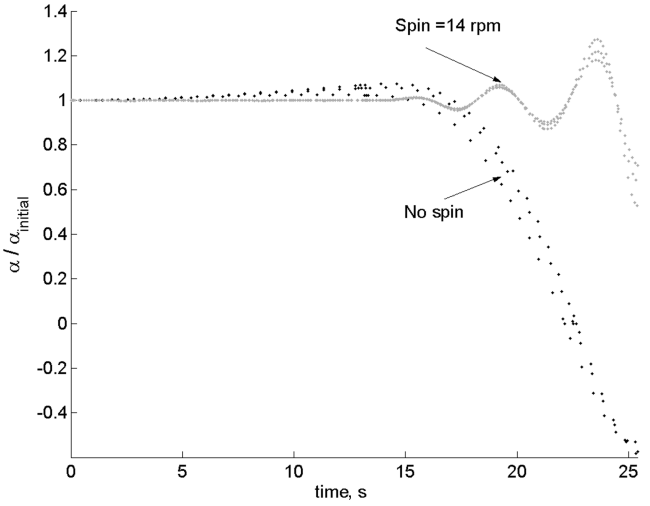

Fig. 5 Time histories of normalized angles of attack for cases in which $\alpha_{\text{init}} = 2$, 7, and 16 deg and $\beta_{\text{init}} = 0$.

IV. Conclusions

In this work, we carried out postflight analysis of the nominal trajectory of Beagle2. We conducted DSMC calculations on the aeroshell, then used the resulting coefficients to conduct a stability analysis in the free-molecular and transition regimes.

The aerodynamic coefficients arising from the DSMC calculations showed that the capsule was unstable in the free-molecular regime and that the aeroshell was only marginally stable at a condition along the nominal trajectory of Beagle2 ($Kn = 0.2846$, time $= 13.2$ s), for which 0 incidence had been targeted indicating that 0 incidence had not been achieved. This effect is similar to that observed in the past and was caused by a high contribution of skin friction to the pitching moment.

With these aerodynamic coefficients, the prescribed spin rate for Beagle2 (85.2 deg/s), which is ideally required to be large enough to counteract the destabilizing moments in the free-molecular regime but not the stabilizing moments in the transition regime, was no longer well matched to the trajectory.

We conducted a dynamic analysis using a diagonalized inertia matrix to ascertain the effect of lower moment coefficients coupled with the high prescribed spin rate.

The results from the dynamic analysis show that the recovery of trim is severely hindered for all cases with initial angles of incidence of 2, 5, 7, 9, 11, and 16.5 deg. This means that the aeroshell was not able to restore trim in the transition regime, a crucial step in the entry and descent phase of the mission. We conclude that it is unlikely that Beagle2 would have traced its nominal trajectory or achieved its target 0 angle of attack condition time $= 13.2$ s due to low moment coefficients induced by a large contribution of skin friction to the moment in the transition regime. This resulted in the high prescribed spin rate for the craft, counteracting the stabilizing moments in the transition regime. We suggest that this was a major reason for the loss of the mission, although more work is needed to prove this.

Acknowledgment

The authors acknowledge Arthur Smith of Fluid Gravity Engineering, Ltd., for obtaining permission for and providing data of the nominal trajectory of Beagle2, as well as its mass and inertia properties, and for insightful discussions.

References

[1] Tsien, H. S., "Superaerodynamics, Mechanics of Rarefied Gases," *Journal of the Aeronautical Sciences*, Vol. 13, No. 12, 1946, pp. 653–664.

[2] Macrossan, M. N., "Scaling Parameters for Hypersonic Flow and the Correlation of Sphere Drag Data," *Proceedings of the 25th International Symposium of Rarefied Gas Dynamics*, edited by M. S. Ivanov and A. K. Rebrov, Publishing House of the Russian Academy of Sciences, Novosibrisk, Russia, 2007, pp. 759–764.

[3] Liever, P.A., Habchi, S. D., Burnell, S. I., Lingard, J. S., and Davis, D. R., "Computational Fluid Dynamics Prediction of the Beagle 2 Aerodynamic Database," *Journal of Spacecraft and Rockets*, Vol. 40, No. 5, 2003, pp. 632–638.

[4] Dahlen, G. A., Macrossan, M. N., Harvey, J. K., and Brundin, C. L., "Blunt Cones in Rarefied Hypersonic Flow: Experiments and Monte-Carlo Simulations," *Proceedings of the 14th International Symposium on Rarefied Gas Dynamics*, edited by H. Ougchi, University of Tokyo Press, Tokyo, 1985, pp. 229–240.

[5] Ivanov, M. S., Markelov, G. N., Gimelshein, S. F., Mishina, L. V., Krylov, A. N., and Grechko, N. V., "High-Altitude Capsule Aerodynamics with Real Gas Effects," *Journal of Spacecraft and Rockets*, Vol. 35, No. 1, 1998, pp. 16–22.

[6] Desai, P. N., Mitcheltree, R. A., and Cheatwood, F. M., "Entry Dispersion Analysis for the Stardust Comet Sample Return Capsule," *Journal of Spacecraft and Rockets*, Vol. 36, No. 3, 1999, pp. 463–469.

[7] Bird, G. A., *Molecular Gas Dynamics and the Direct Simulation of Gas Flows*, Oxford Engineering Science Series, Clarendon, Oxford, 1994.

[8] Zipfel, P. H., *Modeling and Simulation of Aerospace Vehicle Dynamics*, AIAA Education Series, AIAA, Reston VA, 2000.

I. Boyd
Associate Editor